Thin Solid Films 547 (2013) 32–37

Contents lists available at ScienceDirect

Thin Solid Films

journal homepage: www.elsevier.com/locate/tsf

Oxygen effect of transparent conducting amorphous Indium Zinc Tin Oxide films on Polyimide substrate for flexible electrode

Yoon Duk Ko [a], Chang Hun Lee [b], Doo Kyung Moon [c], Young Sung Kim [b,*]

[a] Display Lab, Sungkyunkwan University, Sungkyunkwan Univ. Natural Sciences Campus, Cheoncheon-dong, Jangan-gu, Suwon-si, Gyeonggi-do, 440-746, Republic of Korea
[b] Graduate school of NID Fusion Technology, Seoul National University of Science and Technology, 138 Gongreung-Gil, Nowon-Gu, Seoul, 139-743, Republic of Korea
[c] Department of material chemistry and engineering, Konkuk University, 1 Hwayang-dong, Gwangjin-gu, Seoul 143-701, Republic of Korea

ARTICLE INFO

Available online 22 May 2013

Keywords:
Transparent conductive oxide (TCO)
Indium zinc tin oxide (IZTO)
Flexible electrode

ABSTRACT

This paper discusses the effect of oxygen on the transparent conducting properties and mechanical durability of the amorphous indium zinc tin oxide (IZTO) films. IZTO films deposited on flexible clear polyimide (PI) substrate using pulsed direct current (DC) magnetron sputtering at room temperature under various oxygen partial pressures. All IZTO films deposited at room temperature exhibit an amorphous structure. The electrical and optical properties of the IZTO films were sensitively influenced by oxygen partial pressures. At optimized deposition condition of 3.0% oxygen partial pressure, the IZTO film shows the lowest resistivity of 6.4×10^{-4} Ωcm, high transmittance of over 80% in the visible range, and figure of merit value of $3.6 \times 10^{-3}\ \Omega^{-1}$ without any heat controls. In addition, high work function and good mechanical flexibility of amorphous IZTO films are beneficial to flexible applications. It is proven that the proper oxygen partial pressure is important parameter to enhance the transparent conducting properties of IZTO films on PI substrate deposited at room temperature.

1. Introduction

Recently more technologies for flexible devices are required for e-papers, organic light emitting diodes (OLEDs), polymer light emitting diodes (PLEDs) and other types of flexible photovoltics. These devices require TCO films as electrodes or anode layers. Today, indium tin oxide (ITO) films are widely used as TCO films for rigid devices, but it is inadequate for flexible applications due to its high deposition temperature, rough surface, imperfect work function, and mechanical brittleness. Many of the alternative materials, therefore, have been researched to substitute ITO films, such as an amorphous phase controlled by doped indium oxide films [1,2], conductive polymers [3,4] and carbon nanotubes (CNTs) [5,6]. Among these materials, the transparent conductive properties of amorphous ITO or indium zinc oxide films prepared at low temperature are not sufficiently complete for the application of flexible devices. Conductive polymers and CNTs are also widely reviewed since its outstanding physical properties. However, both of materials are currently not competitive with conventional ITO films for practical applications. For this reason, IZTO films have gained much attention due to its high optical transparency, good conductivity, and high work function compared to ITO films in spite of low deposition temperature [7]. In former studies, IZTO films were generally prepared by a sputtering system, and their characteristics were analyzed with different deposition conditions such as temperature, power, and thickness [8,9]. However, no research has been reported concerning the optimum oxygen partial pressure for deposition for flexible substrate and its mechanical reliability. In this work, we prepared IZTO thin films on flexible clear polyimide (PI) substrate by using pulsed DC magnetron sputtering system with different oxygen partial pressure. Basically, the structural, electrical, and optical properties of IZTO films were examined. Furthermore, we investigated mechanical flexibility and reliability of optimized IZTO films. Based on this research result, we can conclude the amorphous IZTO film deposited at room temperature with its optimum oxygen partial pressure showed comparable resistivity and transparency to those of conventional ITO films. In addition, its smooth surface, high work function, and mechanical bendability also offers many beneficial properties for flexible electrodes. Therefore, IZTO films with optimum deposition conditions can be applied to polymer substrate, and has the advantage of manufacturing flexible displays.

2. Experiment

The IZTO films were deposited on clear PI substrate (Mitsubishi Gas. Chem. Neopulim) by pulsed DC magnetron sputter system. The ceramic target for sputtering was prepared by mixing and sintering 70.0 at.% In_2O_3, 15.0 at.% SnO_2 and 15.0 at.% ZnO powders. The PI substrate with 25 mm × 25 mm size was cleaned in an ultra-sonicator in the order of isopropyl alcohol and de-ionized water. The substrates were dried by blowing N_2 gas, and loaded in the sputtering chamber. The distance between PI substrate and target was kept at 7 cm, where the substrate rotated at the steady speed of 0.25 revs/s in order to obtain homogeneous deposition of films. Then, the chamber was initially evacuated to the basal pressure of 9.3×10^{-5} Pa. The input power and frequency

* Corresponding author. Tel.: +82 2 970 6804; fax: +82 2 970 6011.
E-mail address: youngsk@seoultech.ac.kr (Y.S. Kim).

0040-6090/$ – see front matter © 2013 Elsevier B.V. All rights reserved.
http://dx.doi.org/10.1016/j.tsf.2013.05.069

were 125 W and 30 kHz, respectively. Sputter deposition is carried out at room temperature. The working pressure was maintained at 0.8 Pa with 16 sccm Ar flow and the flow rate of O_2 was varied. The flow ratio of O_2 [$O_2/(O_2 + Ar)$] changes from 0.0 to 4.0% with the fixed total (O_2 + Ar) flow rate. Hereafter, oxygen gas flow ratio will be referred to as oxygen partial pressure. Target was pre-sputtered for 5 min prior to the main deposition to remove contaminant or oxide layer of its surface. The sputtering deposition rates were controlled at 0.48 nm/s. The thickness of the deposited IZTO films was 200 nm, measured with an alpha step of surface profiler (KLA-Tencor 500, U.S.A.).

The crystal structure of the films was analyzed by X-ray diffraction (XRD; D8 ADVANCE, Brunker, Germany) pattern with Cu Kα (λ = 0.1639 nm) radiation collected from theta-2theta scan in the range of 15°–80°, and the crystal phase was reviewed with samples processed by focused ion beam (FIB; NOVA600 NanoLab, FEI, Holland) through high resolution transmission electron microscopy (HRTEM; JEM-2100(HR) + Cs corrector, JEOL/CEOS, Japan). The surface morphology was analyzed by field emission scanning electron microscopy (FESEM; S-4800, HITACHI, Japan) with operating voltage of 15 kV. The electrical properties including the resistivity, carrier concentration and mobility of the IZTO films were measured using the van der Pauw method with Hall measurement system (HMS-3000, ECOPIA, Korea). The transmittance of the films was measured using an ultraviolet (UV)–visible spectrometer (S-3100, SCINCO, Korea) within a wavelength between 200 nm and 1100 nm. The work functions of the films were measured by using an inelastic secondary electron cutoff of ultraviolet photoemission spectroscopy (UPS; AXIS-NOVA, Kratos Inc., England) and calculated from the results of the energy distribution curve.

The change of electrical resistance (ΔR) of the films was measured with a computer-controlled bending test machine and 4-point probe station during the dynamic fatigue bending test to investigate the mechanical reliabilities of the IZTO films deposited on the transparent PI substrate. The dynamic fatigue bending tests were carried out using a cyclic bending test machine at a frequency of 0.5 Hz for the duration of 2000 cycles, and the bending test was performed with two different approaches depending on the stress state subjected on the films.

3. Results and discussion

Fig. 1 shows the X-ray diffraction patterns of IZTO films with various oxygen partial pressures to investigate the structural properties of the films. Regardless of oxygen partial pressure, all XRD plots of the IZTO films show weak and broad representing IZTO layer (~31°) with PI substrate (~16°). All IZTO films show amorphous structure because of the low substrate temperature during sputtering process. The structural stability of the amorphous IZTO films is attributed to the immiscibility

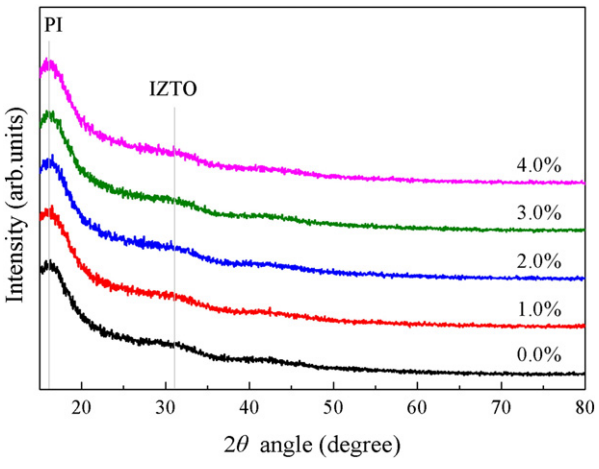

Fig. 1. X-ray diffraction patterns of IZTO thin films deposited at various oxygen partial pressures on PI substrate.

of ZnO and SnO_2 in the In_2O_3 despite the IZTO films were exposed into plasma during the sputtering process [10]. In general, crystallization of SnO_2 doped In_2O_3 film occurs rapidly even at room temperature due to low amorphous/crystalline transition temperature (~150 °C). However, ZnO doped In_2O_3 could maintain a stable amorphous structure below 500 °C due to high amorphous/crystalline transition temperature. Therefore, to make crystalline IZTO films, phase separation of ZnO and SnO_2 from In_2O_3 is necessary. However, the kinetics of phase separation of ZnO and SnO_2 in IZTO film deposited at room temperature are very low. As a result, the IZTO film can maintain a stable amorphous structure.

XRD result suggested that some short range order could be present in the film structure. However, only from the XRD results, we cannot conclude that IZTO structure was purely amorphous. Hence we performed HRTEM on IZTO films. Fig. 2 (a) shows the cross-section HRTEM image with an inset of the selected-area electron diffraction (SAED) pattern of the IZTO film deposited at 3.0% oxygen partial pressure. The uniform contrast of the IZTO film with low porosity indicates that the structure of the IZTO films on PI substrate is amorphous, as expected from the XRD results. The SAED patterns of IZTO films also exhibit a diffused ring pattern indicative of almost amorphous character of the layer. Fig. 2 (b) shows a typical image of the IZTO film where short ranges order under a few nanometers can be evaluated. However, no other distinctive feature resulting from diffraction contrast has been detected in agreement with an essentially amorphous structure.

Surface morphology of the IZTO films deposited on PI substrate as a function of oxygen partial pressure was analyzed by FESEM. Fig. 3 shows surface morphology changes of the IZTO films with various oxygen partial pressures and reference ITO film on PI substrate. It is shown that the reference ITO film on PI substrate has a relatively rough surface due to preferred orientation of the ITO structure [11]. However, the surface of IZTO films with very fine grains is very smooth and featureless without defects such as pinholes, cracks, and protrusion due to the stable amorphous structure of the amorphous IZTO film. The smooth surface of TCO anode film is very important to accomplish high performance of OLEDs or PLEDs because the surface roughness with spikes of the TCO anode can critically affect the breakdown or short circuit of the OLEDs or PLEDs devices [12].

The carrier density (n), carrier mobility (μ) and resistivity (ρ) of the IZTO films were measured from Hall effect measurement system using the Van der Pauw method. Fig. 4 shows the changes in the resistivity, carrier density, and mobility of the IZTO anode films with various oxygen partial pressures on PI substrate. It can be seen that the electrical resistivity has a rapid decrease when the oxygen partial pressure is increased to 3.0%, after that the electrical resistivity starts to increase slightly with the increase of the oxygen partial pressure. The contributions to the carrier density in IZTO films could arise from both the oxygen vacancies V_O^{2+} and the activated Sn^{4+} ions on In^{3+} sites [13]. Since only the oxygen content in the deposition atmosphere was varied in our system, the change of resistivity for IZTO films can be explained by the number of oxygen vacancies as a source of electrical charge carriers in the films. Normally pure or doped In_2O_3 films deposited using ceramic target lose oxygen in sputtering process, and form non-stoichiometric thin films with oxide complex [14]. The high resistivity (~1.8×10^4 Ωcm) of non-stoichiometric IZTO films deposited at no oxygen gas flow could result from the phases of metal oxide in the films. However, with increasing oxygen partial pressure to 2.0%, a proper injection of the oxygen gas during sputtering contributes to the generation of carriers such as oxygen vacancies due to reducing metal oxide complexes in the films [15]. And with further increasing oxygen partial pressure larger than 2.0%, the number of oxygen vacancies decreases, leading to lower carrier density. In addition, the carrier mobility of the IZTO films increased with increasing oxygen partial pressure from 0.0% to 3.5% due to the removal of oxide phases at low oxygen partial pressure (0.0–2.0%) and the decrease of oxygen vacancies acting as scattering centers of free electrons at high oxygen partial pressure (2.5–3.5%) [16,17]. However, the further

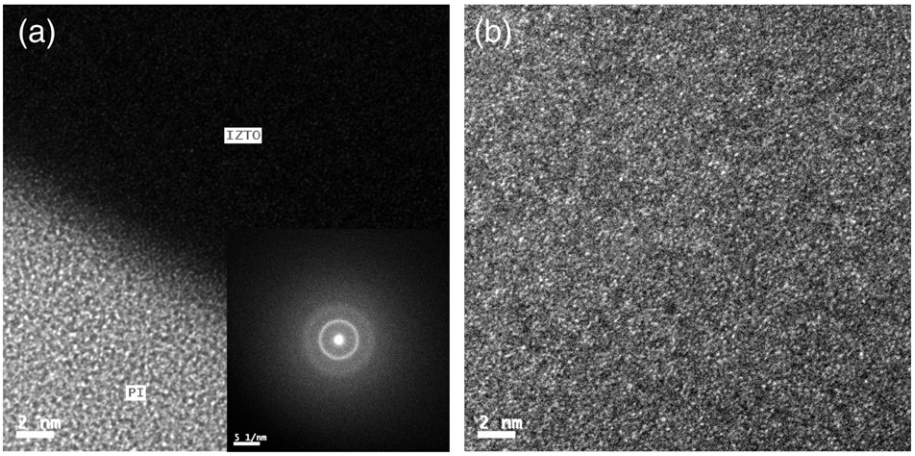

Fig. 2. (a) Cross-sectional HRTEM image with the inset of a SAED pattern, and (b) bright-field image obtained from an IZTO thin film (oxygen partial pressure: 3.0%) grown on PI substrate.

increase of oxygen partial pressure (4.0%) can reduce the carrier mobility since the excess oxygen acting as scattering centers in thin films. As a result, the deposited IZTO film with 3.0% oxygen partial pressure exhibits the lowest resistivity of 6.4×10^{-4} Ωcm. These experimental data shows that the electrical resistivity of the IZTO film is very sensitive to the variation of oxygen partial pressure in sputtering process. Since the electrical resistivity of the IZTO films on PI substrate deposited at room temperature may be comparable to that of conventional ITO thin films deposited at high temperatures, the IZTO thin films on flexible PI substrate at optimum condition can be suitable as an electrode for flexible displays.

Fig. 5 (a) shows the optical transmittance of the IZTO films including PI substrate deposited at various oxygen partial pressures. The IZTO films deposited at no oxygen partial pressure gives a low transmittance in the visible range. As the oxygen partial pressure is increased up to 3.0%, the transmittance of the IZTO films increases as well. However, when the oxygen partial pressure is increased further (3.5 ~ 4.0%), the transmittance in the visible range starts to saturate and decrease. In sputtering process with In_2O_3, ZnO and SnO_2 mixed oxides target, a metal like, dark film of lower oxide will be formed due to loss of oxygen [18]. Therefore, the no or low oxygen partial pressure may not be enough to compensate the loss of the oxygen during the sputtering process and result in a low transmittance. On the other hand, the input of proper oxygen flow can compensate the loss of the oxygen during the sputtering process and result in a high optical transmittance. These clearly show that adding a proper amount of oxygen gas significantly improved the optical transmittance of the IZTO films. The optical transmittance of IZTO films deposited at 3.0% oxygen partial pressure showed higher than 80% including PI substrate which could be obtained for a wavelength in the visible light range.

The optical energy band gap of IZTO films was determined from the plot of $(\alpha h\upsilon)^2$ against $h\upsilon$ by extrapolating the straight line portion of this plot to the energy axis, as shown in Fig. 5(b). As the oxygen partial pressure increases up to 2.0%, the Eg of the IZTO films increases and gets a maximum 3.86 eV due to the Burstein-Moss effect [19,20]. However, oxygen partial pressure further increasing, the band gap decreases, which is due to the carrier concentration effect. Therefore, it is considered that the optical band gap of the IZTO films is related to the change of carrier density in IZTO films with various oxygen partial pressures.

Fig. 6 shows the figure of merit value, average optical transmittance, and sheet resistance of the IZTO films in the wavelength of 400 ~ 800 nm as a function of the oxygen partial pressure. The figure of merit (Φ_{TC}) value can be calculated from Eq. (1), where T is transmittance and R_{sh} is sheet resistance of the IZTO anode films

$$\Phi_{TC} = T^{10}/R_{sh} \quad (1)$$

The Φ_{TC} value, which is suggested by Haacke, is useful for comparing the performance of TCO films with similar transmittance and resistivity [21]. The figure of merit (Φ_{TC}) of IZTO films increase with increasing oxygen partial pressure until 3.0%, as shown in Fig. 6. The increase in the oxygen partial pressure leads to an increase in the Φ_{TC} value of IZTO films with high transmittance and low resistivity. However, for the oxygen partial pressure ≥ 3.5%, the Φ_{TC} value decreases due to the increasing of R_{sheet}. From the evaluated Φ_{TC} value of the IZTO films, it was decided that the optimum oxygen partial pressure for the IZTO films is 3.0%.

It is worth noting that the work function of the TCO films since the device efficiency of the OLEDs or PLEDs devices is very much dependent on the work function of the films which are basically dependent on the surface compositions [22]. High work function electrodes are used to inject holes into the organic materials, hence as high as possible work function values desirable. Work function of IZTO films is measured by using an inelastic secondary electron cutoff of ultraviolet photoelectron spectroscopy (UPS) and calculated from the results of the energy distribution curve. More explicitly it may be stated that the electrons below the Fermi level (E_F^{IZTO}) of IZTO are excited by the UV light of HeI discharge at 21.2 eV, and emitted into vacuum, arbitrarily chosen as vacuum level (E_{vac}^{IZTO}) which is usually the cutoff energy of the UPS spectrum. The kinetic energy distribution of photoelectrons (UPS spectra) expresses the density of the valence states of thin film. The high energy cutoff corresponds to the emission from Fermi level, and the low energy cutoff shows the energy of the vacuum level. From these data the work function (ϕ_{IZTO}) of a film can be determined Eq. (2).

$$\phi_{IZTO} = h\nu(= 21.22\ \text{eV}) - E_{vac}^{IZTO} \quad (2)$$

The work function value of IZTO films deposited with various oxygen partial pressures are shown in Fig. 7. The work function value is increased and saturated from 5.6 eV to 5.9 eV with the increase of the oxygen partial pressure up to 2.0%. It is noted that surface chemical status is related to the work function of doped In_2O_3 thin film; especially an increase of oxygen concentration can increase the work function of films [23,24]. In our study the doping concentration of ZnO and SnO_2 in IZTO film was fixed, and the samples cleaning, preparation method was same to measure the UPS. Therefore the reduction of oxygen vacancies with increasing oxygen partial pressure can increase the work function in IZTO films, which corresponds to the electrical carrier density of the films as shown in Fig. 4. Regardless of the oxygen partial pressure, the work function of all IZTO films (>5.4 ev) is larger than that of ITO films (~4.7 eV).

Fig. 8 shows the inner/outer bending reliability and the fatigue test results of optimized IZTO films deposited at 3.0% oxygen partial pressure. The change in resistance is expressed as ΔR ($= R - R_0$), where

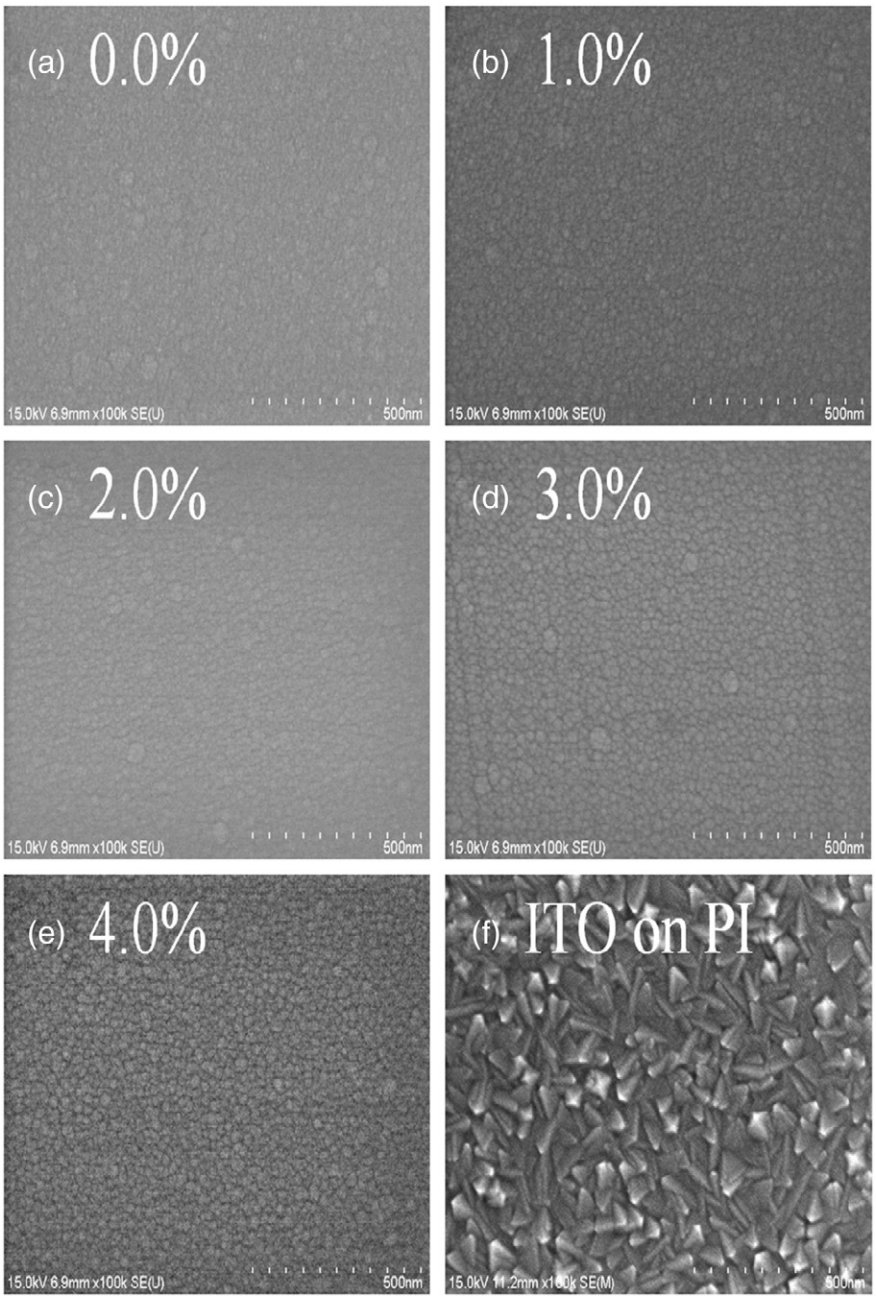

Fig. 3. Surface morphology on (a–e) IZTO thin films with various oxygen partial pressure and (f) reference ITO thin films deposited at room temperature on PI substrate.

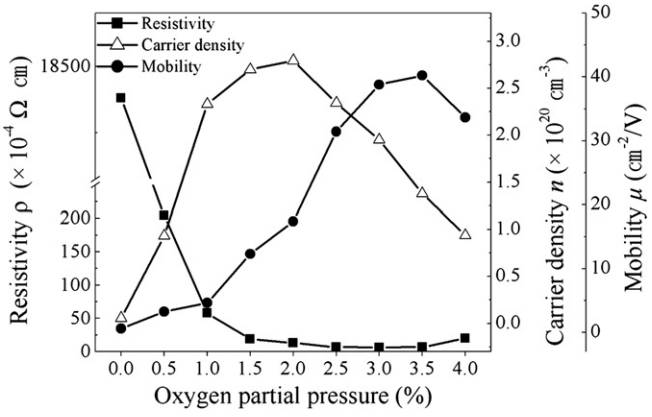

Fig. 4. Variation of the resistivity, the carrier density, and the mobility of IZTO films with different oxygen partial pressures on PI substrate.

R_0 is the initial resistance and R is the measured resistance after bending. From the results of both inner/outer reliabilities of the IZTO films shown Fig. 8, the electrical resistance of the IZTO films does not change up to a bending radius 3.5 mm in inner bending mode and 7.5 mm in outer bending mode, respectively. Yu et al. studied the inner and outer bending reliabilities of ITO films (evaporation source material was a mixed ITO bulk with 90 wt.% In_2O_3 and 10 wt.% SnO_2) with a thickness of 100 nm deposited by an ion beam assisted deposition system method on a PET film (125 °C) [25]. From their research results, the electrical resistance of the ITO film did not change up to a bending radius of 20 mm in inner bending mode and 11 mm in outer bending mode, respectively. In comparing the both bending reliability results of the IZTO films with those of ITO films, it can be obtained that the IZTO films deposited on a PI substrate exhibit an improved reliability over the former ITO films deposited on a PET substrate. This result is intimately linked with the structural difference between polycrystalline ITO

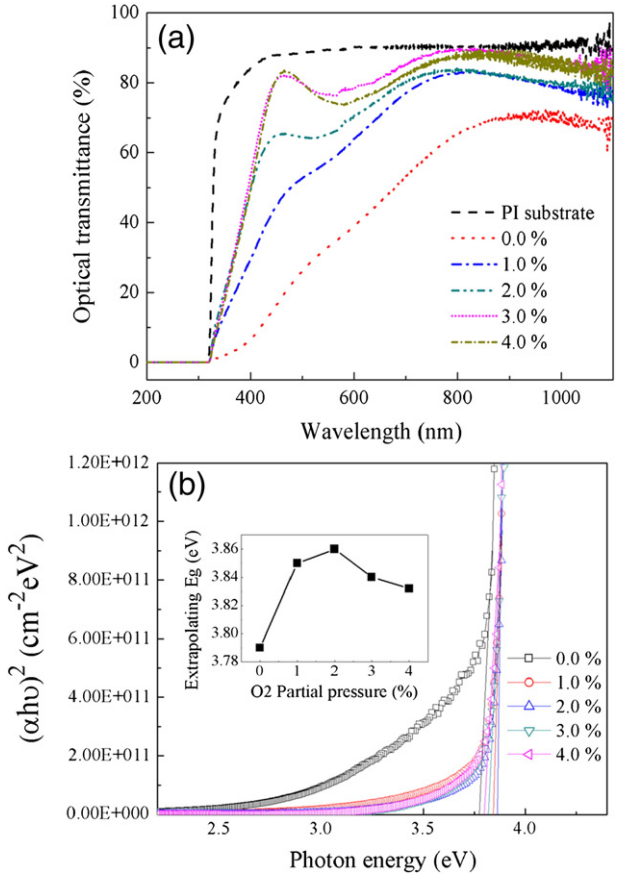

Fig. 5. (a) Optical transmittance spectra, (b) plot of $(\alpha h\upsilon)^2$ vs. photon energy of the IZTO thin films at various oxygen partial pressures on PI substrate.

and amorphous IZTO films. The amorphous IZTO films, as shown in Fig. 1, have robust structure for external force. However, the polycrystalline ITO film is more prone to cracks due to intergranular defects on the grains by external force. The inset of Fig. 8 shows the normalized resistance change after repeated bending for IZTO films deposited at optimized condition (3.0% oxygen partial pressure). The dynamic bending fatigue test was carried out at a frequency of 0.5Hz, 15 mm bending radius over duration of 2000 cycles. During the 2000 cycles of the bending fatigue test, the IZTO films showed excellent mechanical reliability. In the magnified view of the graphs in the each figure indicates that the rate of change of electrical

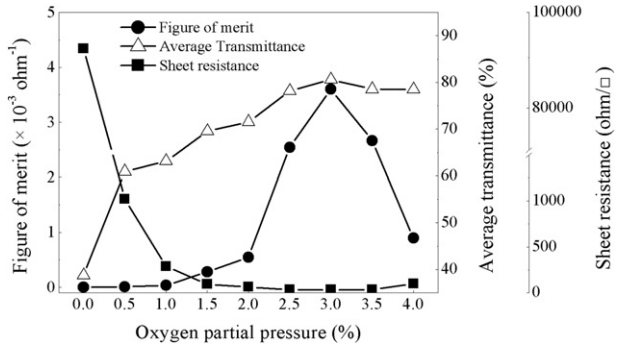

Fig. 6. Calculated figure of merit value for IZTO films grown at various oxygen partial pressure on PI substrate.

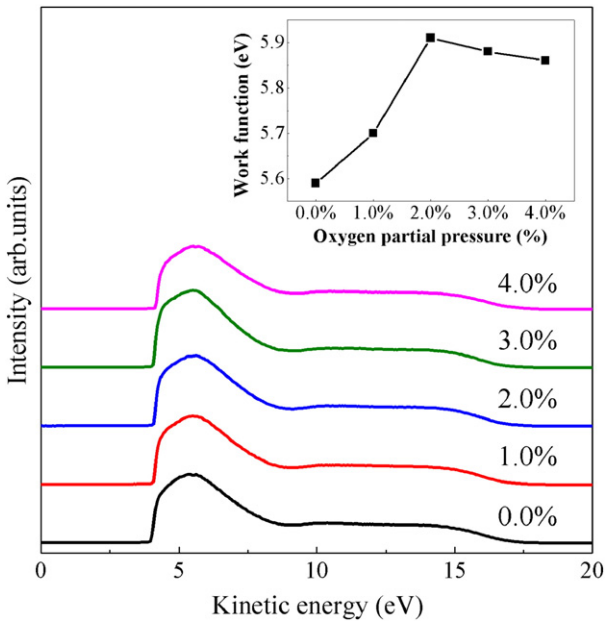

Fig. 7. Low kinetic energy cutoffs of the IZTO films with UPS and the work function of the IZTO films deposited at various oxygen partial pressure on PI substrate.

resistance for the outer bending and the inner bending fatigue tests were less than 1.0% and 0.7%, respectively. As a result, IZTO films with better mechanical durability and reliability can be more

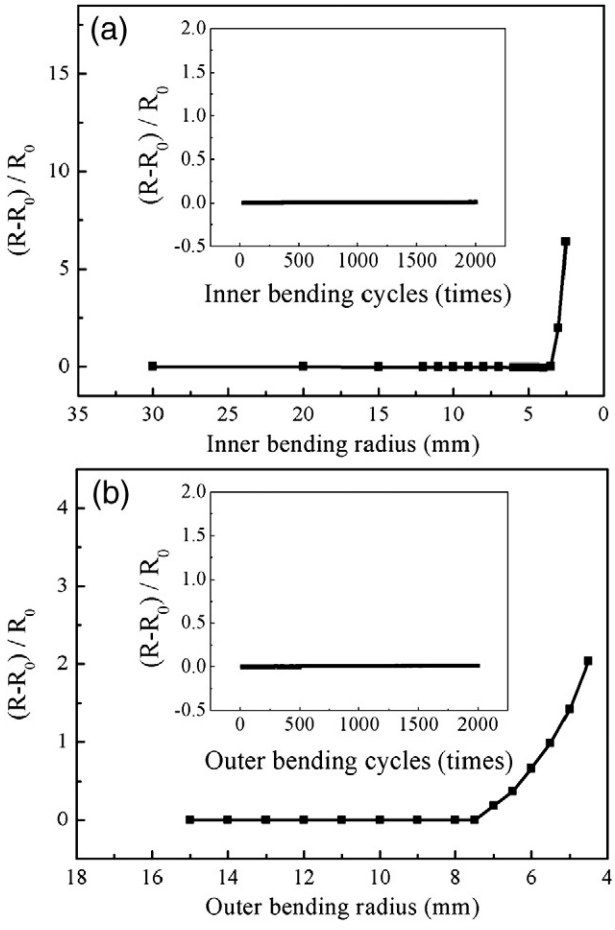

Fig. 8. Comparison of (a) inner and (b) outer bending behavior of IZTO film (oxygen partial pressure: 3.0%) on PI substrate, which insets show normalized resistance change after fatigue bending test.

suitable than conventional ITO films as an anode layer for flexible OLED or PLED devices.

4. Conclusion

Amorphous IZTO films were prepared on flexible clear PI substrate at room temperature by the pulsed DC magnetron sputtering. The IZTO films show a homogeneous and stable amorphous structure regardless of its oxygen partial pressures. However, the amorphous IZTO films with low resistivity and high transmittance could be obtained by adding a proper oxygen gas in sputtering process. At optimized conditions of 3.0% oxygen partial pressure, the amorphous IZTO films show low resistivity of $6.4 \times 10^{-4}\,\Omega$, high optical transmittance of over 80%. The smooth surface morphology and high surface work function of amorphous IZTO films were additionally beneficial to flexible OLEDs or PLEDs. Furthermore, the mechanical reliability and durability of IZTO films shows better performance compared to conventional ITO films because of its amorphous structure. Consequently, these results suggest that IZTO films deposited at room temperature with an optimum deposition condition are suitable to flexible electrode applications for next generation display industry as a substitute for conventional ITO films.

Acknowledgments

This work was supported by the technology supporting project grant funded by the Korean government's Ministry of Knowledge Economy (No.2012K10042360).

References

[1] D.H. Kim, M.R. Park, H.J. Lee, G.H. Lee, Appl. Surf. Sci. 253 (2006) 409.
[2] H.K. Kim, Surf. Coat. Technol. 203 (2008) 652.
[3] Y.M. Chang, L. Wang, W.F. Su, Org. Electron. 9 (2008) 968.
[4] S.I. Na, S.S. Kim, J. Jo, D.Y. Kim, Adv. Mater. 20 (2008) 4061.
[5] Z.C. Wu, Z.H. Chen, X. Du, J.M. Logan, J. Sippel, M. Nikolou, K. Kamaras, J.R. Reynolds, D.B. Tanner, A.F. Hebard, A.G. Rinzler, Science 305 (2004) 1273.
[6] M.W. Rowell, M.A. Topinka, M.D. McGehee, H.J. Prall, G. Dennler, N.S. Sariciftci, L.B. Hu, G. Gruner, Appl. Phys. Lett. 88 (2006) 233506.
[7] J.M. Phillips, R.J. Cava, G.A. Thomas, S.A. Carter, J. Kwo, T. Siegrist, j.J. Krajewski, J.H. Marshall, W.F. Peck Jr., D.H. Rapkine, Appl. Phys. Lett. 67 (1995) 2246.
[8] H.K. Park, J.A. Jeong, Y.S. Park, H.K. Kim, W.J. Cho, Thin Solid Films 517 (2009) 5563.
[9] G.S. Heo, I.G. Gim, J.W. Park, K.Y. Kim, T.W. Kim, J. Solid State Chem. 182 (2009) 2937.
[10] J.H. Bae, J.M. Moon, S.W. Jeong, J.J. Kim, J.W. Kang, D.G. Kim, J.K. Kim, J.W. Park, H.K. Kim, J. Electrochem. Soc. 155 (2008) J1.
[11] R. Tahar, T. Ban, Y. Ohya, Y. Takahashi, J. Appl. Phys. 83 (1998) 2631.
[12] L.S. Hung, C.H. Chen, Mater. Sci. Eng. R. 39 (2002) 143.
[13] C.W. Ow-Yang, H.Y. Yeom, D.C. Paine, Thin Solid Films 516 (2008) 3105.
[14] H.N. Cui, V. Teixeira, L.J. Meng, R. Martins, E. Fortunato, Vacuum 82 (2008) 1507.
[15] B. Yaglioglu, Y.J. Huang, H.Y. Yeom, D.C. Paine, Thin Solid Films 496 (2006) 89.
[16] F.O. Adurodija, H. Izumi, T. Ishihara, H. Yoshioka, H. Matsui, M. Motoyama, Appl. Phys. Lett. 74 (20) (1999) 3059.
[17] S. Naseem, I.A. Pauf, K. Hussain, N.A. Malik, Thin Solid Films 156 (1988) 161.
[18] L.J. Meng, J. Gao, R.A. Silva, S. Song, Thin Solid Films 516 (2008) 5454.
[19] E. Burstein, Phys. Rev. 93 (1954) 632.
[20] T.S. Moss, Proc. Phys. Soc. Lond. Ser. B67 (1954) 775.
[21] G. Haacke, J. Appl. Phys. 47 (1976) 4086.
[22] T. Ishida, H. Kobayashi, Y. Nakato, J. Appl. Phys. 73 (1993) 4344.
[23] Y. Park, V. Choong, Y. Gao, B.R. Hsieh, C.W. Tang, Appl. Phys. Lett. 68 (1996) 2699.
[24] K. Sugiyama, H. Ishii, Y. Ouchi, K. Seki, J. Appl. Phys. 87 (2000) 295.
[25] Z.N. Yu, F. Xia, Y.Q. Li, W. Xue, The Asia Optical Fiber Communication & Optoelectronic Exposition & Conference 2008 (AOE 2008), Shanghai, China, Conference proceedings, October 30 - November 2 2008, p. 1.